UDC 616.23/.25,616.986.988:616.24-002-07-084.001.5

https://doi.org/10.15407/biotech19.01.055

In silico STUDY OF THE ANTICORONAVIRAL ACTIVITY OF ALIPHATIC AMINOCARBOXYLIC COMPOUNDS

M.P. Smetiukh [1, 2]

S.O. Soloviov [1, 2]

[1]Igor Sikorsky Kyiv Polytechnic Institute, Ukraine

[2]Shupyk National University of Health Care of Ukraine, Kyiv

E-mail: msmetiuh@gmail.com

Aim. To evaluate the potential interactions of short-chain aliphatic aminocarboxylic compounds with key coronavirus proteases—the main protease (Mpro) and papain-like protease (PLpro) of SARS-CoV-2 and IBV—using molecular docking.

Methods. Hort-chain aminocarboxylic compounds were used as ligands; initial structures were obtained from PubChem or built in Avogadro/MarvinSketch, followed by 3D optimization, verification of protonation at pH 7.4, correction of charge states, and conversion to .mol2 format (OpenBabel) for compatibility with SwissDock. Docking was performed using experimental 3D structures of Mpro and PLpro of SARS-CoV-2 and IBV from the PDB; structure preparation and analysis were carried out in Avogadro, MarvinSketch, OpenBabel, the PubChem 3D Conformer Generator, SwissDock (EADock DSS/AutoDock Vina), and PyMOL.

Results. Aliphatic aminocarboxylic compounds exhibited moderate binding affinity toward Mpro (ΔG from −3.0 to −4.3 kcal/mol), with docking poses predominantly localized in peripheral hydrophobic pockets rather than stably in the catalytic region. Longer-chain ligands, including 7-aminoheptanoic and 8-aminocaprylic acids, showed more stable binding. Extension of the carbon chain enhanced hydrophobic packing and stabilized binding within an Mpro pocket. The non-ionized form of 6-aminocaproic acid bound more favorably than its hydrochloride, consistent with reduced affinity under strong ionization.

Conclusions: Docking indicated moderate binding and predominantly peripheral localization of complexes. Longer chains improve docking scores, whereas strong ionization impairs binding. Conserved Mpro architecture between SARS-CoV-2 and IBV supports the use of IBV as a safer screening model. The most reliable in vitro candidates were identified as 4-aminobutyric acid and 6-aminocaproic acid.

Keywords: SARS-CoV-2, infectious bronchitis virus, coronavirus, molecular docking, aminocarboxylic compounds, Mpro, antiviral agents, *in silico.*

The recent outbreak of COVID-19, caused by SARS-CoV-2, has posed new public health challenges, including the urgent need for novel antiviral agents. First identified in December 2019 in Wuhan, China, the virus rapidly spread among humans, causing severe respiratory illness with high hospitalization and mortality rates [1, 2]. Working with highly pathogenic viruses such as SARS-CoV-2 requires strict adherence to biosafety regulations and facilities at least at the BSL-3 level [3], which complicates and limits experimental studies, especially during the early stages of drug development. Consequently, the use of model viruses [4] and *in silico* approaches allows preliminary screening of potentially active compounds without direct contact with human pathogens [5, 6]. Among *in silico* techniques, molecular docking is widely applied to predict the spatial orientation and energetic feasibility of interactions between small-molecule ligands and viral protein targets [7, 8].

Citation: Smetiukh, M. P. , Soloviov, S. O. (2026). *In silico* study of the anticoronaviral activity of aliphatic aminocarboxylic compounds. *Biotechnologia Acta*, 19(1), 55–37. https://doi.org/10.15407/biotech19.01.055

Coronaviruses (CoVs) of the Coronaviridae family possess crown-like surface spikes [9] and have the largest genomes among RNA viruses. They encode two polyproteins essential for replication [10]. Key representatives include betacoronaviruses (SARS-CoV, MERS-CoV, SARS-CoV-2) and gammacoronaviruses, such as infectious bronchitis virus (IBV). Virions contain an RNA genome complexed with the N nucleocapsid protein, surrounded by a membrane with structural proteins E and M, and covered by the spike protein S [11–13].

All Orthocoronavirinae encode the four main structural proteins: Spike (S), Envelope (E), Membrane (M), and Nucleocapsid (N) [14]. Among these, the main protease (Mpro/3CLpro), responsible for processing polyproteins into functional non-structural proteins, and the S protein, mediating receptor binding and cell entry, are of particular interest [13, 14].

A substantial structural similarity is observed between the Mpro of beta- and gammacoronaviruses. Specifically, SARS-CoV-2 Mpro shares over 41% amino acid identity and approximately 55% primary-sequence similarity with IBV Mpro, including the conserved catalytic dyad His41 and Cys145 [15]. Moreover, the functional similarity of the papain-like proteases of IBV and SARS-CoV-2, particularly their shared ability to perform deubiquitination, further highlights the relatedness of these viruses.

Due to the conservation of key viral proteins, safe, nonpathogenic strains such as IBV can serve as model viruses for preliminary antiviral research. Prior in vitro studies on Vero and BHK-21 cell cultures demonstrated that a series of aliphatic amino compounds exhibited antiviral activity against IBV [16]. Understanding their potential mechanisms of action at the molecular level is enabled by molecular docking, which identifies binding sites for these compounds with key IBV proteins.

This study aimed to perform molecular docking to identify and analyze potential binding sites of aliphatic aminocarboxylic compounds with key coronavirus proteins, primarily Mpro and PLpro.

Seven low-molecular-weight compounds structurally similar to γ- and ω-amino acids were used in the study: 4-aminobutyric acid (GABA), 5-aminovaleric acid, 6-aminocaproic acid, 6-aminocaproic acid hydrochloride, 7-aminoheptanoic acid, 8-aminocaprylic acid, and methyl 6-aminocaproate hydrochloride.

Primary structural data for the listed compounds were obtained from the PubChem database when a validated 3D conformer was available for each molecule. For compounds that lacked an appropriate 3D record, initial structures were built manually in Avogadro and MarvinSketch, followed by generation and optimization of three-dimensional geometry using the PubChem 3D conformer generation service.

The degree and pattern of protonation of all molecules were checked according to the physiological environment commonly accepted in most viral enzyme models — pH 7.4. When necessary, the charge and valence states of functional groups were adjusted (mainly $-NH_2/NH_3^+$ and $-COOH/COO^-$). To ensure compatibility with the SwissDock computational engine, all structures were converted into the .mol2 format, which accurately preserves atom types, formal charges, and stereochemistry. Conversion was performed using OpenBabel with an additional check for geometric artifacts.

Experimental three-dimensional structures of enzymes from two coronaviruses — Infectious Bronchitis Virus (IBV) and SARS-CoV-2 — obtained from the Protein Data Bank (PDB) were used in the study.

For each virus, two key non-structural proteins (nsps) associated with polyprotein processing were analyzed main protease (Mpro, 3CLpro) and papain-like protease (PLpro). For SARS-CoV-2, several Mpro structures were used, including apo forms and the wild type, reflecting catalysis in its natural state. This approach made it possible to account for potential variability in the conformations of the active site (Table 1).

Software and working environment

The following tools were used for structure preparation: Avogadro 1.2 — molecular construction and basic optimization; MarvinSketch (ChemAxon) — protonation check and charge specification; OpenBabel 3.1.1 — format conversion and geometry control; PubChem 3D Conformer Generator — optimized conformers with minimized energy; SwissDock — docking using the EADock DSS method with automated generation of global and local search spaces on the SwissDock platform — AutoDock Vina; PyMOL — additional visualization of complexes [17, 18].

After obtaining the results, internal scripts were used for visualization and clustering of conformations, calculation of interatomic distances, and analysis of interaction types (hydrogen bonds, electrostatic contacts, salt

Table 1. **Key viral proteins and their predicted functions with structural targets**

Virus	Protein	Predicted function	Target
IBV	Main protease (Mpro)	Catalytic cleavage of polyproteins	2Q6D
IBV	Papain-like protease (PLpro)	Polyprotein processing, immunomodulation	4X2Z
SARS-CoV-2	Main protease (Mpro)	Proteolytic processing of polyproteins (with the Q256A mutation)	9GHN
SARS-CoV-2	Papain-like protease (PLpro)	Polyprotein processing, immune antagonism	9CSY

bridges, van der Waals interactions). For each complex, a blind docking mode was applied to avoid bias regarding the localization of the binding site.

ADME analysis and target prediction

For each ligand, the following parameters were calculated: LogP [19], TPSA [20], gastrointestinal absorption (GI absorption) [21], and BBB permeability (SwissADME); possible biological targets using SwissTargetPrediction [22, 23].

Results and Discussion

Binding energy and ligand localization (docking)

Docking against SARS-CoV-2 Mpro and PLpro revealed a clear target-dependent binding pattern and a limited number of preferred binding environments. Overall, most ligands displayed moderate predicted affinities, while a subset repeatedly adopted well-defined poses in recurring pockets, supporting non-random localization rather than diffuse surface adsorption.

For SARS-CoV-2 Mpro, the most favorable scores were obtained for 8-aminocaprylic acid ($\Delta G = -4.307$ kcal/mol) and 4-aminobutyric acid ($\Delta G = -4.290$ kcal/mol) (Fig. 1). Both ligands were placed within inner pocket regions, consistent with a binding mode driven by a combination of polar anchoring and hydrophobic packing. Notably, several ligands converged on the same pocket microenvironment, repeatedly involving LYS5, SER284, LEU282, and GLU288 (with additional contacts such as TYR126 and GLN127 for 8-aminocaprylic acid). This recurrent residue set suggests a stable pocket architecture that can accommodate small polar ligands while maintaining favorable nonpolar contacts.

A strong contrast was observed for 6-aminocaproic acid hydrochloride (6ACA_HCl), which produced consistently weak docking scores against both SARS-CoV-2 proteases (approximately –1 kcal/mol) and was frequently annotated as being located "inside the protein," a placement typically interpreted as non-productive under standard docking assumptions. This pattern supports the view that strongly ionized salt forms are less compatible with predominantly hydrophobic subpocket environments and incur unfavorable desolvation penalties, thereby reducing the likelihood of stable, functionally relevant binding under the applied conditions (Table 2).

Molecular docking against IBV Mpro and IBV PLpro indicated predominantly moderate binding energies for the aminocarboxylic compounds, with a small number of ligands standing out as the most consistent performers for each target (Table 2). For IBV

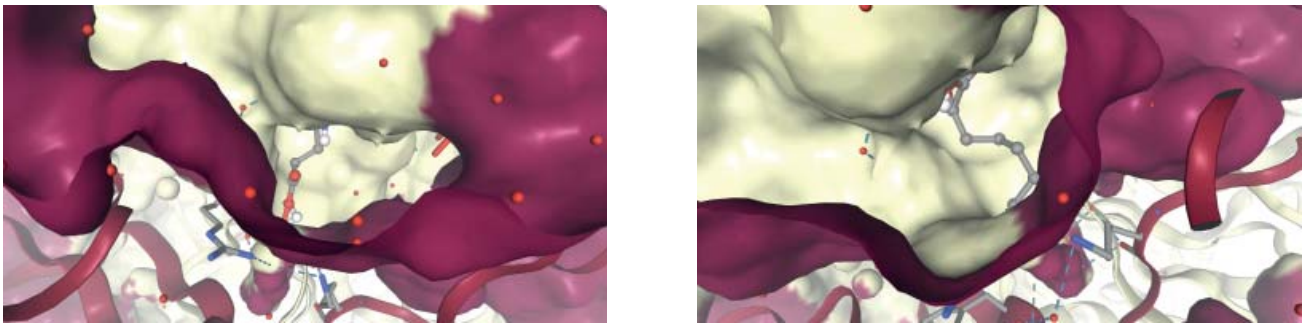

Fig. 1. **Ligand localization in SARS-CoV-2 Mpro**

Table 2. **Molecular docking results of ligands with viral protein targets**

Ligand	Target	ΔG (kcal/mol)	Binding site	Main contacting residues	Comment
1	22	3	4	5	6
5-aminovaleric acid	9GHN	-3.609	Surface	PHE3, LYS5, SER284, GLU288, LEU282	On the surface, slightly embedded
5-aminovaleric acid	9CSY	-3.497	Surface	GLU124, ILE123, TYR136, LEU120	On the surface, slightly embedded
5-aminovaleric acid	2Q6D	-3.978	Pocket	LYS5, LYS4	In a pocket, deep within the protein
5-aminovaleric acid	4X2Z	-3.770	Surface	ASN160, HIS164, TRP156	On the surface, slightly embedded
6-aminocaproic acid	9GHN	-3.762	Pocket	LEU282, TRP207, GLY283, GLU288, PHE3, VAL291	Good affinity
6-aminocaproic acid	9CSY	-3.752	Surface	LEU125, ILE123, TYR136, GLN121, LEU120	On the surface, slightly embedded
6-aminocaproic acid	2Q6D	-3.770	Surface	GLN307, ARG305, GLY141, TYR116, SER137, PHE138	On the surface, slightly embedded
6-aminocaproic acid	4X2Z	-3.534	Surface	LEU67, TRP139, HIS164, GLU163, ASN160, LYS71, GLY66	On the surface, slightly embedded
6-aminocaproic acid hydrochloride	2Q6D	-0.928	Inside the protein	PRO166, LEU169	Very weak
6-aminocaproic acid hydrochloride	9GHN	-0.995	Inside the protein	MET6, GLN299, ASP295	Poor binding
6-aminocaproic acid hydrochloride	9CSY	-1.078	Inside the protein	TYR264	Very weak
6-aminocaproic acid hydrochloride	4X2Z	-1.081	Inside the protein	HIS164, TYR64	Very weak
7-aminoheptanoic acid	9GHN	-3.699	Inner pocket	HOH728, PHE3, LEU282, SER284, GLU288, LYS5	Moderate affinity
7-aminoheptanoic acid	9CSY	-3.492	Surface pocket	LEU120, TYR136, GLU124, GLN122	Moderate affinity
7-aminoheptanoic acid	2Q6D	-3.589	Surface pocket	GLY141, GLN307, HIS170, TYR116, VAL304	Moderate affinity
7-aminoheptanoic acid	4X2Z	-3.780	Surface pocket	TRP156, CYS144, ASN160, GLU163, HIS164	Moderate affinity
8-aminocaprylic acid	9GHN	-4.307	Pocket	LYS5, HOH538, TYR126, GLN127, ARG4, SER284, LEU282, GLU288	Good pocket accommodation, numerous hydrogen bonds
8-aminocaprylic acid	9CSY	-3.890	Pocket	TYR136, LEU125, GLN121, GLY100, THR102	Moderate affinity
8-aminocaprylic acid	2Q6D	-3.940	Surface pocket	CYS143, HIS41, GLY44, ASN25, LEU43	Moderate affinity
8-aminocaprylic acid	4X2Z	-3.534	Surface pocket	GLU163, HIS164, ASN160, GLY66, LYS71	Moderate affinity
4-aminobutyric acid	9CSY	-3.210	Surface	TYR207, ARG166, VAL202, MET206	On the surface, slightly embedded

Table 2 (End)

1	22	3	4	5	6
4-aminobutyric acid	9GHN	-4.290	Inner pocket	CYS128, GLN127, ARG4, HOH672, LYS5	The ligand is positioned inside the inner pocket
4-aminobutyric acid	2Q6D	-3.742	Surface	TYR166, GLY303, GLU164, TYR116	On the surface, slightly embedded
4-aminobutyric acid	4X2Z	-3.557	Surface	SER143, ASN160, HIS164	On the surface, slightly embedded
Methyl 6-aminocaproate hydrochloride	9GHN	-3.675	Pocket	SER284, LEU282, TRP207, LYS5, PHE3, ILE281, GLU288	Moderate affinity
Methyl 6-aminocaproate hydrochloride	9CSY	-3.504	Pocket	LEU125, TYR136, LEU120, GLN121	Moderate affinity
Methyl 6-aminocaproate hydrochloride	2Q6D	-3.554	Pocket	TYR116, GLY141, GLU164, GLN307, HOH438	Moderate affinity
Methyl 6-aminocaproate hydrochloride	4X2Z	-3.204	Surface pocket	HIS164, GLY66, SER143	On the surface, in a small depression

Note. Surface binding — ligand interaction with the external protein surface without significant invasion into shallow pockets. Peripheral pocket — a shallow local depression near the protein surface allowing partial ligand accommodation. Catalytic center (active site) — the region comprising the catalytic dyad His41 and Cys145 (SARS-CoV-2 Mpro numbering) and spatially associated catalytic residues.

Mpro, the strongest scores were obtained for 5-aminovaleric acid and 8-aminocaprylic acid (Fig. 2). Although their predicted affinities were close, 8-aminocaprylic acid was notable because its top pose included contacts in the active-site region (His41/Cys143 in the main protease IBV numbering), which is more suggestive of functionally relevant binding than broadly distributed surface adsorption.

Most of the remaining ligands clustered in the intermediate range and were typically positioned in surface or peripheral pockets, consistent with stabilization driven by mixed polar and weak hydrophobic contacts rather than a tightly locked catalytic-site pose. In contrast, the hydrochloride salt form (6-aminocaproic acid hydrochloride) consistently produced poor docking scores for both IBV proteases. It was frequently annotated as occupying an "inside the protein" location, a pattern commonly interpreted as non-productive binding under standard docking assumptions. This supports the conclusion that strong ionization is unfavorable in this system, likely reducing compatibility with hydrophobic subpockets and penalizing desolvation.

For IBV PLpro, the highest-scoring ligands were 7-aminoheptanoic acid and 5-aminovaleric acid, which repeatedly localized to a preferred surface-pocket region centered on ASN160/HIS164. The recurrence of this contact environment—often accompanied by an aromatic contribution (e.g., TRP156 in top poses)—suggests a dominant binding region in PLpro that anchors ligands through a combination of polar interactions and local hydrophobic/aromatic stabilization. Overall, these results nominate 5-aminovaleric acid and 8-aminocaprylic acid as the most supported candidates for IBV Mpro (with 8-aminocaprylic acid showing the most active-site–proximal pattern), and 7-aminoheptanoic acid and 5-aminovaleric acid as the most consistent binders for IBV PLpro, while strongly ionized salt forms remain the least favorable under the applied docking conditions.

Physicochemical profiling of the ligand series

All investigated compounds fully comply with Lipinski's rule of five and do not exhibit physicochemical outliers, indicating their overall drug-like character and allowing the exclusion of trivial factors, such as excessive molecular size, polarity, or lipophilicity, as drivers of the observed docking and cellular assay results (Table 3). Under these

conditions, differences in target binding and biological activity can be reasonably attributed to molecular structural features rather than to fundamental limitations of their physicochemical profiles.

The TPSA values for most ligands fall within a narrow range (~63 Å^2), indicating a high degree of chemical homogeneity within the series and enabling a reliable comparative analysis of molecular docking results. At the same time, TPSA values of this magnitude are characteristic of relatively polar molecules, which favors predominantly surface or peripheral docking poses dominated by hydrogen bonding and electrostatic interactions, rather than deep insertion into hydrophobic subpockets of the protein.

The most informative distinction within the series is the gradual increase in iLOGP with elongation of the aliphatic chain, reflecting enhanced hydrophobic packing within target binding sites and correlating with more favorable binding energies for 7-aminoheptanoic acid and 8-aminocaprylic acid. In this context, 6-aminocaproic acid hydrochloride stands out due to its highly hydrophilic profile, which may limit its compatibility with hydrophobic pockets. In contrast, methyl 6-aminocaproate hydrochloride exhibits an intermediate interaction profile, combining sufficient polarity with moderate lipophilicity but lacking the maximal contribution of hydrophobic contacts observed for the longer-chain derivatives.

To place the docking results in a broader biological context, we performed a comparative analysis with experimental *in vitro* data obtained from cell-based assays. Overall, the *in silico* and *in vitro* datasets exhibit partial, target- and compound-dependent concordance rather than a simple rank-order correlation. Docking against IBV proteases (Mpro and PLpro) yielded predominantly moderate predicted affinities across the ligand series, whereas the cellular readouts reflect a composite outcome of intrinsic antiviral activity, effective cellular exposure, and cytotoxicity, quantified by CD50 and CTI under different treatment regimens. Consequently, several compounds displaying only moderate docking scores nevertheless demonstrated measurable antiviral effects in vitro, while others with comparatively favorable docking profiles did not translate into meaningful antiviral indices within non-toxic concentration ranges.

Importantly, molecular docking in the present study is applied as a mechanistic, hypothesis-generating approach intended to identify plausible ligand binding modes, interaction patterns, and protein interaction hot spots. In this context, the observed discrepancies between docking outcomes and in vitro performance underscore the multifactorial nature of cellular antiviral activity and highlight the limitations of docking as a standalone predictor of *in vitro* efficacy.

Interpretation of the cell-based results also benefits from basic ADME context. SwissADME predictions indicate that all tested molecules show zero Lipinski violations and broadly similar TPSA values, reducing the likelihood that differences in CTI are driven by gross physicochemical constraints such as excessive size or polarity. At the same time, ionization state and lipophilicity can strongly influence the behavior of amino-acid–like compounds in cellular systems, which is consistent with the poorest overall profiles observed for hydrochloride salt forms. Interpretation of the cell-based results also benefits from basic ADME context. SwissADME predictions indicate that all tested molecules show zero Lipinski violations

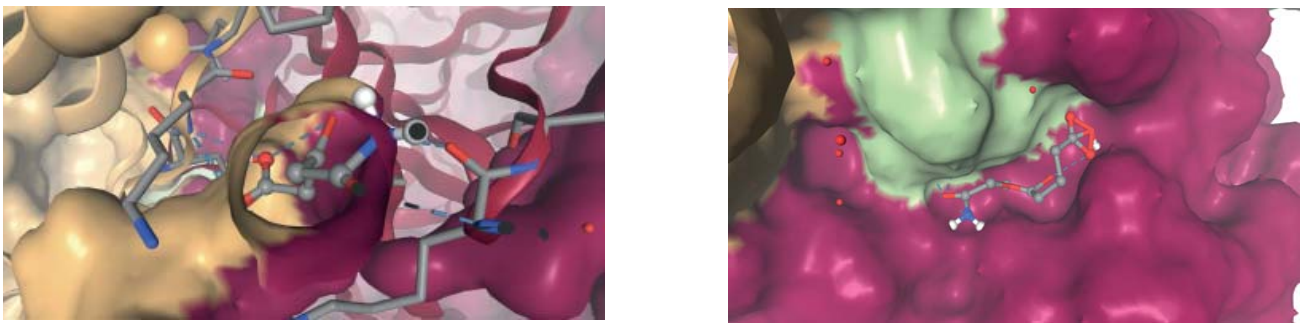

Fig. 2. **Ligand localization in IBV Mpro**

Table 3. **Physicochemical properties of the studied ligands**

Ligand	Lipinski's rules	Topological polar surface area (TPSA, Å²)	Log Po/w (iLOGP)
4-aminobutyric acid	Yes, 0 violations	63.32	0.72
5-aminovaleric acid	Yes, 0 violations	63.32	0.98
6-aminocaproic acid hydrochloride	Yes, 0 violations	63.32	0.00
7-aminoheptanoic acid	Yes, 0 violations	63.32	1.41
8-aminocaprylic acid	Yes, 0 violations	63.32	1.47
6-aminocaproic acid	Yes, 0 violations	63.32	1.20
methyl 6-aminocaproate hydrochloride	Yes, 0 violations	52.32	0.75

and broadly similar TPSA values, reducing the likelihood that differences in CTI are driven by gross physicochemical constraints such as excessive size or polarity. At the same time, ionization state and lipophilicity can strongly influence the behavior of amino-acid–like compounds in cellular systems, which is consistent with the poorest overall profiles observed for hydrochloride salt forms Interpretation of the cell-based results also benefits from basic ADME context. SwissADME predictions indicate that all tested molecules show zero Lipinski violations and broadly similar TPSA values, reducing the likelihood that differences in CTI are driven by gross physicochemical constraints such as excessive size or polarity. At the same time, ionization state and lipophilicity can strongly influence the behavior of amino-acid–like compounds in cellular systems, which is consistent with the poorest overall profiles observed for hydrochloride salt forms. In this sense, ADME assessment supports the conclusion that docking is most reliable for negative selection (discarding forms unlikely to achieve productive binding or a usable therapeutic window), while positive *in vitro* performance depends strongly on exposure and tolerability.

Two compounds— 4-aminobutyric acid and 6-aminocaproic acid —were the most consistent performers in the cell model, combining high CD50 values with reproducible CTI positivity in the therapeutic and treatment modes. In docking, both compounds showed only moderate, predominantly surface/peripheral placements against IBV Mpro/PLpro, suggesting that their cellular antiviral signal is unlikely to be explained solely by a tightly locked, deeply buried active-site complex with the viral proteases. This pattern is consistent with either weak-to-moderate protease engagement that becomes detectable *in vitro* because of a favorable exposure/toxicity window, and/or additional host-mediated contributions not captured by docking.

By contrast, 8-aminocaprylic acid illustrates a common disconnect in early antiviral screening: it ranked among the better docking solutions (including contacts in the active-site region of IBV Mpro in the Mpro numbering), yet produced only a limited in vitro signal that was mainly apparent as a late treatment effect. 5-aminovaleric acid showed a similar delayed profile, where strong docking to IBV Mpro did not translate into broad CTI positivity. Finally, the hydrochloride salt forms—most clearly 6-aminocaproic acid hydrochloride and methyl 6-aminocaproate hydrochloride — showed the most straightforward agreement between approaches: docking yielded very weak energies and frequently non-productive placements, while in vitro they exhibited high cytotoxicity that likely collapsed the therapeutic window and prevented measurable antiviral indices. Taken together, these findings support prioritizing 4-aminobutyric acid and 6-aminocaproic acid as the most reliable in vitro leads, while treating docking primarily as a mechanistic hypothesis generator rather than a standalone predictor of cellular antiviral efficacy.

Conclusions

Aliphatic amino-containing compounds investigated in this study generally exhibit moderate affinity toward coronavirus proteases (approximately ΔG −3.0 to −4.3 kcal/mol) and reproducibly localize to a limited number of dominant binding regions. For most ligands, peripheral or surface binding within hydrophobic pockets or shallow surface depressions is characteristic, whereas

stable positioning directly within the Mpro catalytic center (His41–Cys145) is not typical. Accordingly, docking data alone do not provide sufficient grounds to claim reliable competitive inhibition of the catalytic sites across the entire compound series.

The results also establish a practical rationale for prioritization: elongation of the aliphatic chain is accompanied by an increase in iLOGP and, consequently, improved hydrophobic packing within binding pockets, which is consistent with more favorable docking energies observed for 7-aminoheptanoic and 8-aminocaprylic acids. In contrast, comparison of 6ACA forms demonstrated that strong ionization is unfavorable: the non-ionized (free) form shows superior binding capacity, whereas hydrochloride salts are characterized by a pronounced reduction in affinity, reflecting limited compatibility with hydrophobic subpockets and reduced stability of docking poses. All compounds remain within the drug-like chemical space (zero Lipinski's rule-of-five violations); therefore, differences in the behavior of the series are more plausibly explained by structural nuances (chain length, ionization state) rather than by gross physicochemical outliers.

Although PLpro docking revealed recurring surface-binding regions, the resulting binding modes and energies were less indicative of stable catalytic-site engagement than those for Mpro. Therefore, PLpro results are considered complementary to the primary focus on Mpro. Structural conservation of Mpro between SARS-CoV-2 and IBV supports IBV as a safe model for primary antiviral screening and mechanistic analysis of protease interactions.

At the same time, comparison of *in silico* and in vitro data underscores that docking-predicted binding does not necessarily translate into cellular antiviral efficacy, which is influenced not only by potential target engagement but also by compound exposure and tolerability within the cellular system. In this context, the results support prioritizing 4-aminobutyric acid and 6-aminocaproic acid as the most promising in vitro candidates within the studied series. At the same time, molecular docking should primarily be regarded as a tool for mechanistic interpretation and for early exclusion of non-productive binding modes rather than as a standalone predictor of cellular antiviral activity.

Funding

State registration No 0123U100390, National Academy of Medical Sciences of Ukraine State Institution "National Scientific Center of Phthisiology, Pulmonology and Allergology named after F. G. Yanovsky of the National Academy of Medical Sciences of Ukraine" TO DEVELOP DIFFERENTIATED MEASURES FOR THE TREATMENT OF PATIENTS WITH LUNG DISEASE OF CORONAVIRUS ETIOLOGY AT VARIOUS STAGES OF THE DISEASE

Conflicts of Interest

The authors declare no conflicts of interest. This article does not contain any human or animal studies conducted by any of the authors.

Author Contributions

Smetiukh M. — paper writing, literature review, data analysis, figure preparation; Soloviov S. — editing, conceptualized the study.

REFERENCES

1. Lai, C. C., Liu, Y. H., Wang, C. Y., Wang, Y. H., Hsueh, S. C., Yen, M. Y., Ko, W. C., Hsueh, P. R. (2020). Asymptomatic carrier state, acute respiratory disease, and pneumonia due to severe acute respiratory syndrome coronavirus 2 (SARS-CoV-2): Facts and myths. *J. Microbiol. Immunol. Infect.*, 53(3), 404412. https://doi.org/10.1016/j.jmii.2020.02.012
2. Wu, C., Liu, Y., Yang, Y., Zhang, P., Zhong, W., Wang, Y., Wang, Q., Xu, Y., Li, M., Li, X., Zheng, M., Chen, L., Li, H. (2020). Analysis of therapeutic targets for SARS-CoV-2 and discovery of potential drugs by computational methods. *Acta Pharm. Sin. B.*, 10(5), 766–788. https://doi.org/10.1016/j.apsb.2020.02.008.
3. Kaufer, A. M., Theis, T., Lau, K. A., Gray, J. L., Rawlinson, W.D. (2020). Laboratory biosafety measures involving SARS-CoV-2 and the classification as a Risk Group 3 biological agent. *Pathology*, 52(7), 790–795. https://doi.org/10.1016/j.pathol.2020.09.006
4. Smetiukh, M. P., Trokhimenko, O. P., Soloviov, S. O., Dziublyk, I. V., Kamatskyi, O. A.,

Savchuk, I. V., Bobyr, N. A. (2024). Biotechnological system for the search of substances with potential activity against coronavirus. *Biotechnologia Acta,* 17(6), 45–55. https://doi.org/10.15407/biotech17.06.045.

5. Murgueitio, M.S., Bermudez, M., Mortier, J., Wolber, G. (2012). *In silico* virtual screening approaches for anti-viral drug discovery. *Drug Discov Today Technol.,* 9(3), e219-25. https://doi.org/10.1016/j.ddtec.2012.07.009
6. Kirchmair. J., Distinto, S., Liedl, K. R., Markt, P., Rollinger, J. M., Schuster, D., Spitzer, G. M., Wolber, G. (2011). Development of antiviral agents using molecular modeling and virtual screening techniques. *Infect. Disord. Drug. Targets,* 11(1), 64–93. https://doi.org/10.2174/187152611794407782.
7. Purohit, P., Borah, P., Hazarika, S., Joshi, G., Deb, P. K. (2023). Computational Modeling in the Development of Antiviral Agents. In: Kar, S., Leszczynski, J. (eds) Current Trends in Computational Modeling for Drug Discovery. *Challenges and Advances in Computational Chemistry and Physics*, 35. Springer, Cham. https://doi.org/10.1007/978-3-031-33871-7_4
8. Berg T. (2003). Modulation of protein-protein interactions with small organic molecules. *Angew. Chem. Int. Ed. Engl.,* 42(22), 2462–2481. https://doi.org/10.1002/anie.200200558
9. Peele, K. A., Potla Durthi, C., Srihansa, T., Krupanidhi, S., Ayyagari, V. S., Babu, D. J., Indira, M., Reddy, A. R., Venkateswarulu, T. C. (2020). Molecular docking and dynamic simulations for antiviral compounds against SARS-CoV-2: A computational study. *Inform. Med. Unlocked,* 19, 100345. https://doi.org/10.1016/j.imu.2020.100345
10. Zmasek, C. M., Lefkowitz, E. J., Niewiadomska, A., Scheuermann, R. H. (2022). Genomic evolution of the Coronaviridae family. *Virology,* 570, 123–133. https://doi.org/10.1016/j.virol.2022.03.005
11. Bhuiyan, M. S. A., Amin, Z., Rodrigues, K. F., Saallah, S., Shaarani, S. M., Sarker, S., Siddiquee, S. (2021). Infectious Bronchitis Virus (Gammacoronavirus) in Poultry Farming: Vaccination, Immune Response and Measures for Mitigation. *Vet. Sci.,* 8(11), 273. https://doi.org/10.3390/poultry2030027
12. Wu, W., Cheng, Y., Zhou, H., Sun, C., Zhang, S. (2023). The SARS-CoV-2 nucleocapsid protein: its role in the viral life cycle, structure and functions, and use as a potential target in the development of vaccines and diagnostics. *Virol. J.,* 20(1), 6. https://doi.org/10.1186/s12985-023-01968-6
13. Yadav, R., Chaudhary, J. K., Jain, N., Chaudhary, P. K., Khanra, S., Dhamija, P., Sharma, A., Kumar, A., Handu, S. (2021). Role of Structural and Non-Structural Proteins and Therapeutic Targets of SARS-CoV-2 for COVID-19. *Cells,* 10(4), 821. https://doi.org/10.3390/cells10040821
14. Yang, H., Rao, Z. (2021). Structural biology of SARS-CoV-2 and implications for therapeutic development. *Nat. Rev. Microbiol.,* 19(11), 685–700. https://doi.org/10.1038/s41579-021-00630-8
15. Semenyuta, I. V., Trokhimenko, O. P., Dziublyk, I. V., Soloviov, S. O., Trokhymchuk, V.V., Bororova, O. L., Hodyna, D. M., Smetiukh, M. P., Yakovenko O. K., Metelytsia, L. O. (2022). Decamethoxin virucidal activity: *in vitro* and in silico studies. *Ukr. Biochem. J.,* 94(3), 81–91. https://doi.org/10.15407/ubj94.03.081
16. Dziublyk, I. V., Soloviov, S. O., Trokhimenko, O. P., Dziublyk, O. Y., Smetiukh, M. P., Yakovenko, O. K.,Vasylenko, V., Sidorenko, M., Mickevicius, S., Gumeniuk, M.I. (2023). In vitro Study of the Spectrum Antiviral Activity of Aliphatic Acid toward the Prototype Coronavirus Strain. *Biomedical and Biotechnology Research Journal* 7(2), 218–224, https://doi.org/10.4103/bbrj.bbrj_36_23
17. Bugnon, M., Röhrig, U. F., Goullieux, M., Perez, M. A. S., Daina, A., Michielin, O., Zoete, V. (2024). SwissDock 2024: major enhancements for small-molecule docking with Attracting Cavities and AutoDock Vina. *Nucleic Acids Res.,* 52(W1), W324–W332. https://doi.org/10.1093/nar/gkae300
18. Eberhardt, J., Santos-Martins, D., Tillack, A. F., Forli, S. (2021). AutoDock Vina 1.2.0: New Docking Methods, Expanded Force Field, and Python Bindings. *J. Chem. Inf. Model.,* 61(8), 3891–3898. https://doi.org/10.1021/acs.jcim.1c00203.
19. Daina, A., Michielin, O., Zoete, V. (2014). iLOGP: a simple, robust, and efficient description of n-octanol/water partition coefficient for drug design using the GB/SA approach. *J. Chem. Inf. Model.*, 2014 Dec 22, 54(12), 3284–3301. https://doi.org/10.1021/ci500467k.
20. Ertl, P., Rohde, B., Selzer, P. (2000). Fast calculation of molecular polar surface area as a sum of fragment-based contributions and its application to the prediction of drug transport properties. *J. Med. Chem.,* 43(20), 3714–4717. https://doi.org/10.1021/jm000942e
21. Daina, A., Zoete, V. (2016). A BOILED-Egg To Predict Gastrointestinal Absorption and Brain Penetration of Small Molecules. *Chem. Med. Chem.,* 11(11), 1117–1121. https://doi.org/10.1002/cmdc.201600182
22. Daina, A., Michielin, O., Zoete, V. (2019). SwissTargetPrediction: updated data and new features for efficient prediction of

protein targets of small molecules. *Nucl. Acids Res.,* 47(W1), W357–W364. https://doi.org/10.1093/nar/gkz382
23. Daina, A., Zoete, V. (2024). Testing the predictive power of reverse screening to infer drug targets, with the help of machine learning. *Comms. Chem.*, 7(1), 105. https://doi.org/10.1038/s42004-024-01179-2
24. Lipinski, C. A., Lombardo, F., Dominy, B. W., Feeney, P. J. (2001). Experimental and computational approaches to estimate solubility and permeability in drug discovery and development settings. *Adv. Drug. Deliv. Rev.,* 46(1–3), 3–26. https://doi.org/10.1016/s0169-409x(00)00129-0.

In silico ДОСЛІДЖЕННЯ АНТИКОРОНАВІРУСНОЇ АКТИВНОСТІ АЛІФАТИЧНИХ АМІНОКАРБОНОВИХ СПОЛУК

Сметюх М.П.[1, 2], *Соловйов С.О.*[1, 2]

[1]Київський політехнічний інститут ім. Ігоря Сікорського, Україна
[2]Національний університет охорони здоров'я України імені П. Л. Шупика, Київ

E-mail: msmetiuh@gmail.com

Мета. Оцінити потенційні взаємодії коротколанцюгових аліфатичних амінокарбонових сполук із ключовими протеазами коронавірусів — основною протеазою (Mpro) та папаїнподібною протеазою (PLpro) SARS-CoV2- і IBV — методом молекулярного докінгу.

Методи. Як ліганди використано коротколанцюгові амінокарбонові сполуки. Вихідні структури отримували з PubChem або будували в Avogadro/MarvinSketch, виконували 3D-оптимізацію, перевірку протонування при pH 7,4, корекцію зарядових станів і конвертацію в формат .mol2 (OpenBabel) для сумісності зі SwissDock. Докінг проводили з експериментальними 3D-структурами Mpro і PLpro SARS-CoV2- та IBV із PDB; підготовку й аналіз структур здійснювали в *Avogadro, MarvinSketch, OpenBabel, PubChem 3D Conformer Generator, SwissDock (EADock DSS/AutoDock Vina)* та *PyMOL*.

Результати. Аліфатичні амінокарбонові сполуки демонстрували помірну спорідненість до Mpro (ΔG від 3,0 до 4,3 ккал/моль), причому їхні пози докінгу переважно локалізувалися в периферійних гідрофобних кишенях, а не стабільно в каталітичній ділянці. Ліганди з довшим ланцюгом, зокрема 7-аміногептанова та 8-амінокаприлова кислоти, показали стабільніше зв'язування. Аліфатичні амінокарбонові сполуки виявили помірну спорідненість до Mpro (ΔG – 3,0–4,3 ккал/моль), причому пози переважно локалізувалися в периферійних гідрофобних кишенях. Подовження вуглецевого ланцюга посилювало гідрофобне пакування та стабілізувало зв'язування в кишені Mpro. Показано, що неіонізована 6-амінокапронова кислота зв'язувалася краще за гідрохлорид, що узгоджується зі зниженням афінності при сильній іонізації

Висновки. Докінг показав помірне зв'язування та переважно периферійну локалізацію комплексів. Довші ланцюги покращували докінг-оцінки, а сильна іонізація погіршувала зв'язування. Консервативність Mpro між SARS-CoV-2 та IBV підтримувало використання IBV як безпечнішої скринінгової моделі. Найбільш надійними *in vitro* кандидатами визначено 4-аміномасляну та 6-амінокапронову кислоти.

Ключові слова: SARS-CoV-2, вірус інфекційного бронхіту, коронавірус, молекулярний докінг, амінокарбонові сполуки, Mpro, противірусні сполуки, *in silico*.

Received 2025/12/30
Revised 2026/01/28
Accepted 2026/02/12